Molecular Microbiology (2011) 79(2), 402–418 ■
doi:10.1111/j.1365-2958.2010.07450.x
First published online 16 November 2010

Nucleoid-associated PhaF phasin drives intracellular location and segregation of polyhydroxyalkanoate granules in *Pseudomonas putida* KT2442

B. Galán,[1] N. Dinjaski,[1] B. Maestro,[2] L. I. de Eugenio,[1] I. F. Escapa,[1] J. M. Sanz,[3] J. L. García[1] and M. A. Prieto[1]*

[1]*Department of Environmental Biology, Centro de Investigaciones Biológicas, CSIC, C/Ramiro de Maeztu, 9, 28040 Madrid, Spain.*
[2]*Instituto Universitario de Electroquímica, Universidad de Alicante, 03080- Alicante, Spain.*
[3]*Instituto de Biología Molecular y Celular, Universidad Miguel Hernández, 03202-Elche, Spain.*

Summary

The PhaF is a nucleoid-associated like protein of *Pseudomonas putida* KT2442 involved in the polyhydroxyalkanoate (PHA) metabolism. Its primary structure shows two modular domains; the N-terminal PHA granule-binding domain (phasin domain) and the C-terminal half containing AAKP-like tandem repeats characteristic of the histone H1 family. Although the PhaF binding to PHA granules and its role as transcriptional regulator have been previously demonstrated, the cell physiology meaning of these properties remains unknown. This work demonstrates that PhaF plays a crucial role in granule localization within the cell. TEM and flow cytometry studies of cells producing granules at early growth stage demonstrated that PhaF directs the PHA granules to the centre of the cells, forming a characteristic needle array. Our studies demonstrated the existence of two markedly different cell populations in the strain lacking PhaF protein, i.e. cells with and without PHA. Complementation studies definitively demonstrated a key role of PhaF in granule segregation during the cell division ensuring the equal distribution of granules between daughter cells. *In vitro* studies showed that PhaF binds DNA through its C-terminal domain in a non-specific manner. All these findings suggested a main role of PhaF in PHA apparatus through interactions with the segregating chromosome.

Accepted 28 October, 2010. *For correspondence. E-mail auxi@cib.csic.es; Tel. (+34) 918373112; Fax (+34) 915360432.

Introduction

Many proteins like histone H1 have the ability to bind to a variety of DNA sequences, the recognition of which depends on some general rather than specific features of the DNA molecule (Bustin *et al*., 2005). The eukaryotic histone H1 is involved in the condensation of chromatin and in blocking access to nucleosomal DNA (Zlatanova *et al*., 2000; Kasinsky *et al*., 2001). This is achieved mainly by the electrostatic neutralization of the negative charges on the linker DNA connecting adjacent nucleosomes. Consequently, these proteins show a positively charged DNA-binding region built up from four to five amino acid stretches with high content of lysine and alanine residues usually interspersed by a proline residue, resulting in a proline-kinked AK α-helix organization which is referred to as the AKP helix (Kasinsky *et al*., 2001). This motif appears to have compositional similarity to some of the histone H1-like proteins from bacteria. The best-characterized members of this group of prokaryotic proteins are probably AlgP and AlgR3 from *Pseudomonas aeruginosa* strain PAO and *P. aeruginosa* strain 8882 respectively (Deretic and Konyecsni, 1990; Kato *et al*., 1990; Deretic *et al*., 1992). These two homologous proteins are known to participate in the full transcriptional activation of the *algD* gene encoding the key biosynthetic enzyme guanosine diphospho-D-mannose dehydrogenase and contain 45 and 40 repeat units of the consensus AAKP tetrapeptide (interspersed with AAKTA pentapeptide) sequences in their C-terminal domain respectively (Medvedkin *et al*., 1995).

A prokaryotic protein containing this AKP helix region within its sequence is the PhaF phasin from *Pseudomonas* species (Timm and Steinbüchel, 1992; Valentin *et al*., 1998; Prieto *et al*., 1999; Moldes *et al*., 2004) (Fig. 1). According to primary structure analyses, PhaF is organized in two domains: (i) the highly positive charged histone like domain at C-terminal half, containing eight AAKP-like tandem repeats, and (ii) the N-terminal part that share sequence similarity with the rest of the phasin family (Prieto *et al*., 1999; Moldes *et al*., 2004). Phasins are located on the surface of the bacterial polyhydroxyalkanoate (PHA) granules, bacterial polyesters accumulated

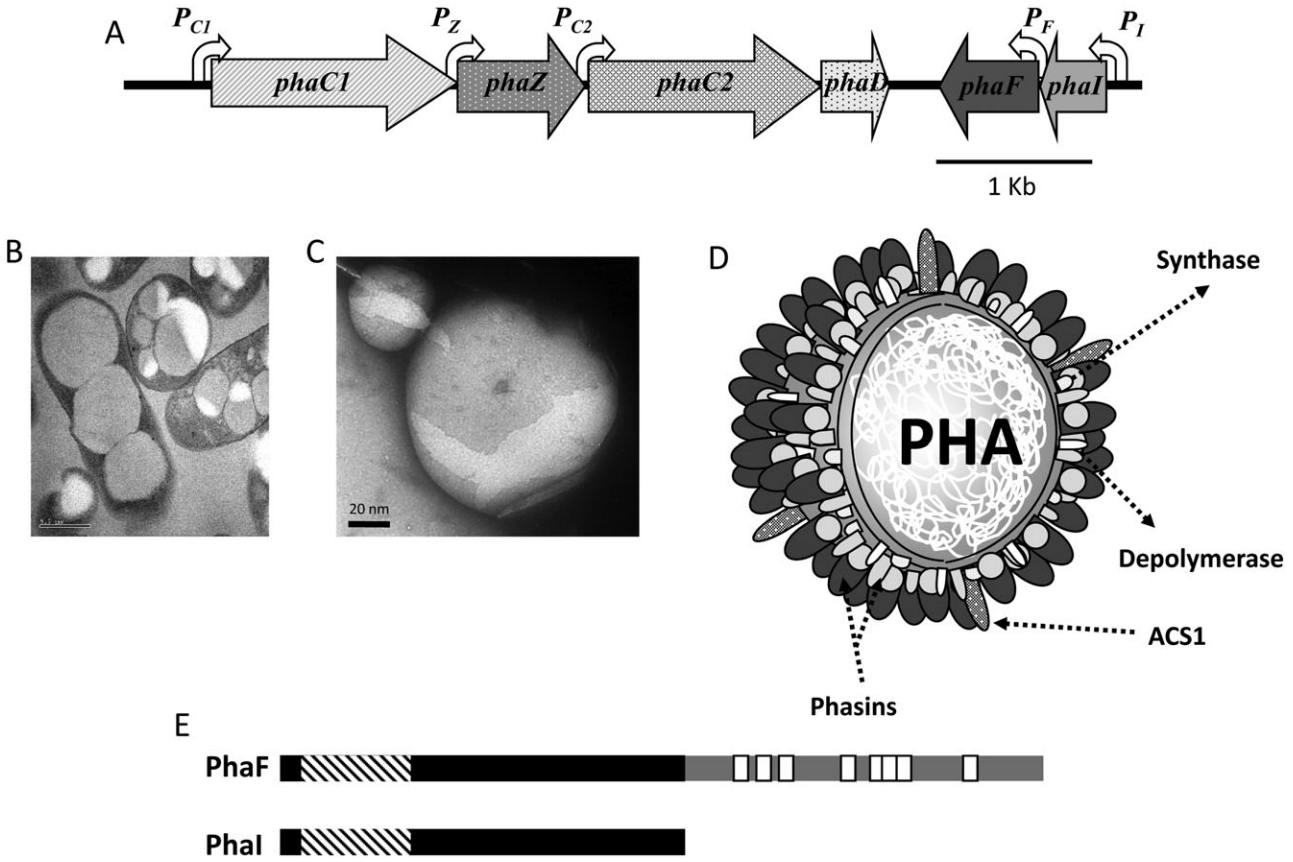

Fig. 1. *pha* gene cluster organization, granule structure and scheme of phasins domains in *P. putida* KT2442.
A. Genetic organization of *pha* cluster, in *P. putida* KT2442. The open arrows indicate the directions of gene transcription. The *phaC1* and *phaC2* genes encode two synthases and are separated by the *phaZ* gene that encodes an intracellular depolymerase. *phaD* gene encodes a transcriptional regulator. *phaF* and *phaI* genes code for phasins. Promoter regions are indicated as curved white arrows.
B. TEM image of mcl-PHA-producing cells of *P. putida* KT2442.
C. TEM image of a PHA granule from *P. putida* KT2442.
D. Model of PHA granule structure. Granules are composed of PHA coated by a monolayer of phospholipids and granule associated proteins (GAPs). The most abundant GAPs are phasins. Polymerases (or synthases), depolymerases and acyl CoA synthetase (ACS1) are also associated to the granule.
E. Domain architecture of the phasins PhaF and PhaI. The N-terminal domain of PhaF is similar to PhaI protein. Hatched and white boxes indicate the putative granule binding sites and the AAKP repeated motifs respectively.

in the cytoplasm as reserve storage granules that are believed to play a role as sink for carbon and reducing equivalents when other nutrients are limited (Madison and Huisman, 1999; Steinbüchel and Hein, 2001; Moldes *et al*., 2004; O'Leary *et al*., 2005). Phasins are thought to generate an interphase between the cytoplasm and the hydrophobic core of PHA granules, preventing them from coalescence (Steinbüchel *et al*., 1995). They also play a role in controlling the size and the number of the granules per cell (Pieper-Fürst *et al*., 1995; Wieczorek *et al*., 1995; Grage *et al*., 2009). In the case of medium-chain-length PHA (mcl-PHA) granules from pseudomonads, formed by hydroxyalkanoic acid monomers consisting of 6–14 carbon atoms, two phasins PhaF and PhaI have been identified as the major granule-associated proteins (Prieto *et al*., 1999). The PhaF N-terminal domain shows 57% of similarity to the complete amino acid sequence of the protein PhaI (Fig. 1E) and it is responsible for the granule binding (Moldes *et al*., 2004). Previous studies performed in *Pseudomonas putida* GPo1 (formerly *Pseudomonas oleovorans* GPo1) demonstrated a bi-functional role for the PhaF protein, as phasin, showing structural function linked to the N-terminal domain (Moldes *et al*., 2004), and as transcriptional regulator, a function very likely related to the histone-like C-terminal domain but not demonstrated yet (Prieto *et al*., 1999). PhaF minus mutants showed increased *pha* cluster transcription rate when cells were cultured in batch fermentation, while PHA content remained unaltered. However, in continuous culture, that is, when cell division and PHA formation occurred simultaneously, the lack of PhaF phasin affected considerably the PHA content of the cells (Prieto *et al*., 1999).

In this work a functional analysis was performed to investigate the role of phasin PhaF in the PHA metabolism, cell physiology and transcriptional regulation of the *pha* genes in the model mcl-PHA producer strain *P. putida* KT2442. Moreover, we demonstrate that PhaF binds DNA unspecifically and it plays a role in the equal distribution of PHA granules between daughter cells during cell division.

Results

PhaF affects heterogeneity of the cell population concerning the PHA production

Previous results from our laboratory showed that the total PHA content of a PhaF mutant strain of *P. putida* GPo1 was reduced considerably in comparison with that of wild-type strain when the PHA content was studied in cell dividing continuous culture (Prieto *et al*., 1999). Based on this observation, we focus our interest in studying the PHA production not only at stationary phase but throughout the growth curve to analyse PhaF-dependent variation in terms of PHA content in all fermentation stages. With this aim, the *phaF* gene of the prototype PHA producer strain *P. putida* KT2442 was deleted by using a suicide vector (see *Experimental procedures*). The PHA production abilities of the resulting strain *P. putida* KT42F was compared with that of the wild-type bacterium when cultured in optimal PHA production conditions. To monitor the PHA content at every stage of the growth curve, a fast and accurate method for analysis of PHA content by flow cytometry was adapted in this work for *Pseudomonas* strains based on a method described previously (Toy *et al*., 2006) (see *Experimental procedures* for details) (Fig. 2).

Cells from *P. putida* KT2442 and its *phaF*-disrupted mutant strain KT42F were harvested from the culture at different growth times. Figure 2A shows that at the early exponential phase of growth (2 h and 4 h), wild-type and mutant strains showed similar PHA content, around 10% and 20% of cell dry weight (CDW) respectively. After 6 h of growth the total PHA content detected in the wild-type strain KT2442 was slightly higher than that of the mutant strain KT42F. This difference increased over the growth curve, being maximal (1.5-fold) after 24 h of growing (Fig. 2A). This result demonstrates that PhaF is not essential for the synthesis of PHA in *P. putida* KT2442 but contributes to optimize the yield of PHA synthesis and accumulation.

Besides, flow cytometry analyses allow us to relate the total PHA content of the cell population versus the PHA content of individual cells (heterogeneity of the population). Figure 2B shows an example of a histogram of KT42F and wild-type cells after 7 h of growing. A major overlay corresponding to positive fluorescent cells was detected in the wild-type cells (Fig. 2B), demonstrating a homogeneous population regarding the PHA granules content. Interestingly, two main overlays showing different fluorescence intensities (Fig. 2B) were detected in the KT42F sample. In this case, only 55% of cell population displayed positive PHA content while the rest of the cells were negative, suggesting that they did not contain PHA granules (Fig. 2C). These results demonstrated the presence of at least two different cell populations in terms of PHA content in the KT42F cultures suggesting a role of PhaF in PHA granules partition during cell division.

Role of PhaF on granule location and segregation during cell division

To monitor the presence of the PHA granules during cell division at early growth phase and the influence of the PhaF protein on the PHA content, samples from wild-type and KT42F mutant strains were taken at different growth times for TEM analysis (Figs 3 and 4). Interestingly, cells at time zero, that is, LB-grown cells used to inoculate the cultures (see *Experimental procedures*), contain a few and small granules of PHA which constitute less than 1% of the CDW (Figs 3A and 4A). In perfect correlation with the PHA content (Fig. 2A), the size and number of the PHA granules in the wild-type cells increased progressively during the growth curve being maximal at 24 h of growing (Fig. 3). Most of the cells contained five to six granules of about 500 nm of diameter (Fig. 5). The number and average size of the granules in the KT42F mutant are decreased when compared with those of the wild-type strain (Fig. 5). These results confirmed those obtained by flow cytometry, which showed a remarkable heterogeneity on the total population in the KT42F culture in terms of PHA content and the presence of PHA empty cells when PhaF protein is not produced.

TEM studies also provided additional information about granule distribution in the cell, and we observed that after 2 h and 4 h of growing, granules were detected in the wild type at the centre of the cross-section of the majority of the cells, i.e. located running lengthwise the cell, forming a characteristic needle array (Fig. 3B, C and F). This distribution was less evident when the accumulation of PHA was close to the 50% CDW after 6 h of growing (Fig. 3D and E). In contrast, the granules in the KT42F mutant strain were agglomerated (Fig. 4B, C and F) at the early times (2 h and 4 h) in one of the cell poles. In agreement with the results observed by flow cytometry (Fig. 2), the PHA content of the mutant was similar to that of the wild-type strain at the earliest stages of growth (Fig. 4B, C and F). Moreover, at 24 h of growth 34% of mutant cells did not contain PHA granules generating two markedly different cell populations in the culture, i.e. with and without PHA (Figs 2B and 4E). While wild-type strain

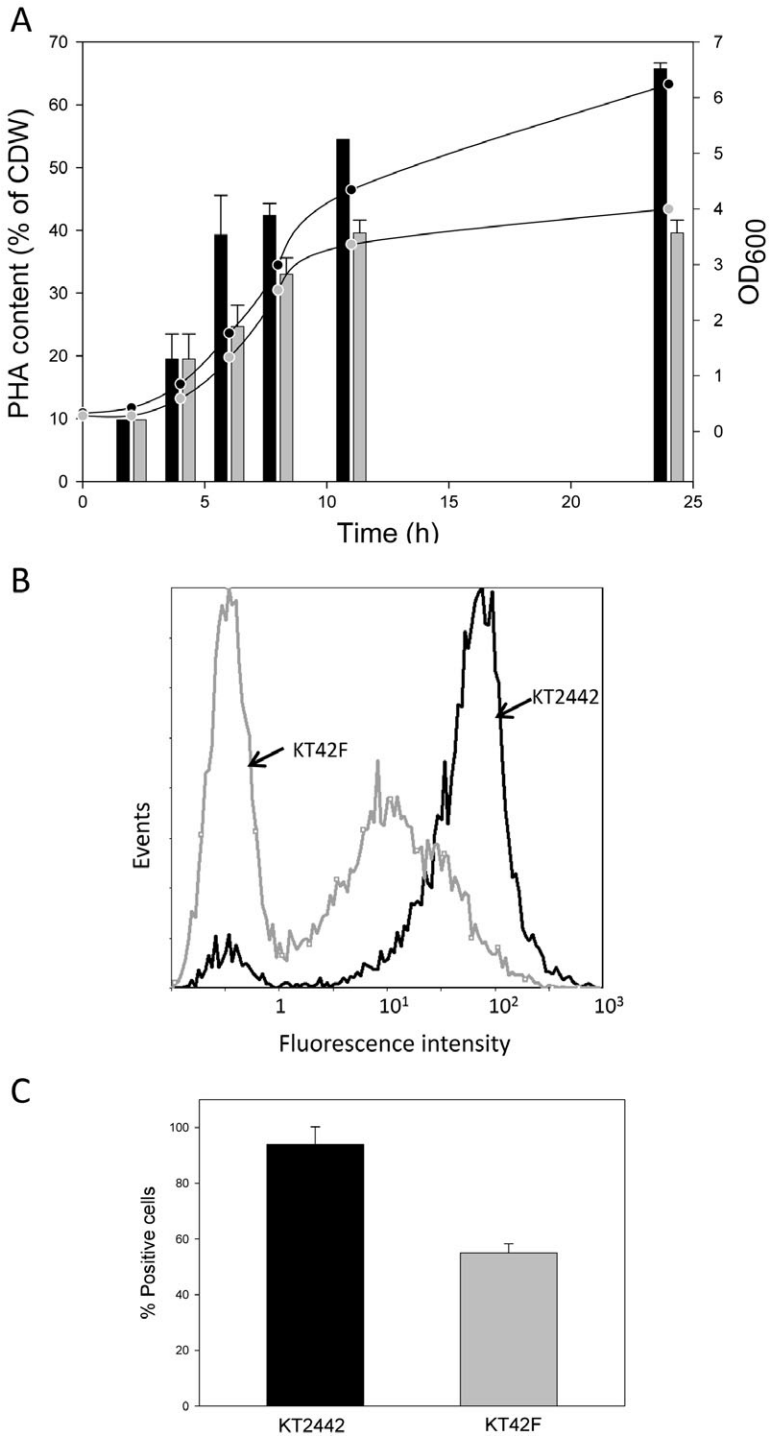

Fig. 2. Study of cell population heterogeneity in terms of PHA production by flow cytometer.
A. Quantification of PHA content (bars) and OD_{600} (circles) of *P. putida* KT2442 (black bars and black circles) and KT42F (grey bars and grey circles) strains throughout the growth curve.
B. Example of a flow cytometer histogram of the *P. putida* KT2442 (black plot) and the *P. putida* KT42F (grey plot) strains grown in PHA production medium during 7 h (see *Experimental procedures* for details).
C. Percentage of PHA-positive cells KT2442 (black column) and KT42F (grey column).

distributed the previously formed PHA granules among the daughter cells keeping the needle array structure, the PHA granules in the PhaF mutant strain remained agglomerated in one of the daughter cells (Fig. 6). It is worth noting that granules did not coalesce in a single big granule, as reported for other microorganism lacking phasins (Wieczorek *et al.*, 1995), very likely due to the presence of the other phasin PhaI (data not shown). On the other hand, *P. putida* KT42F cells were complemented by *in trans* production of PhaF from *P. putida* GPo1 giving rise to *P. putida* KT42F-F strain (see *Experimental procedures* for details) (Fig. 6). These results demonstrated that the presence of PhaF ensures the segregation of the PHA granules during the cell division. Moreover, we have

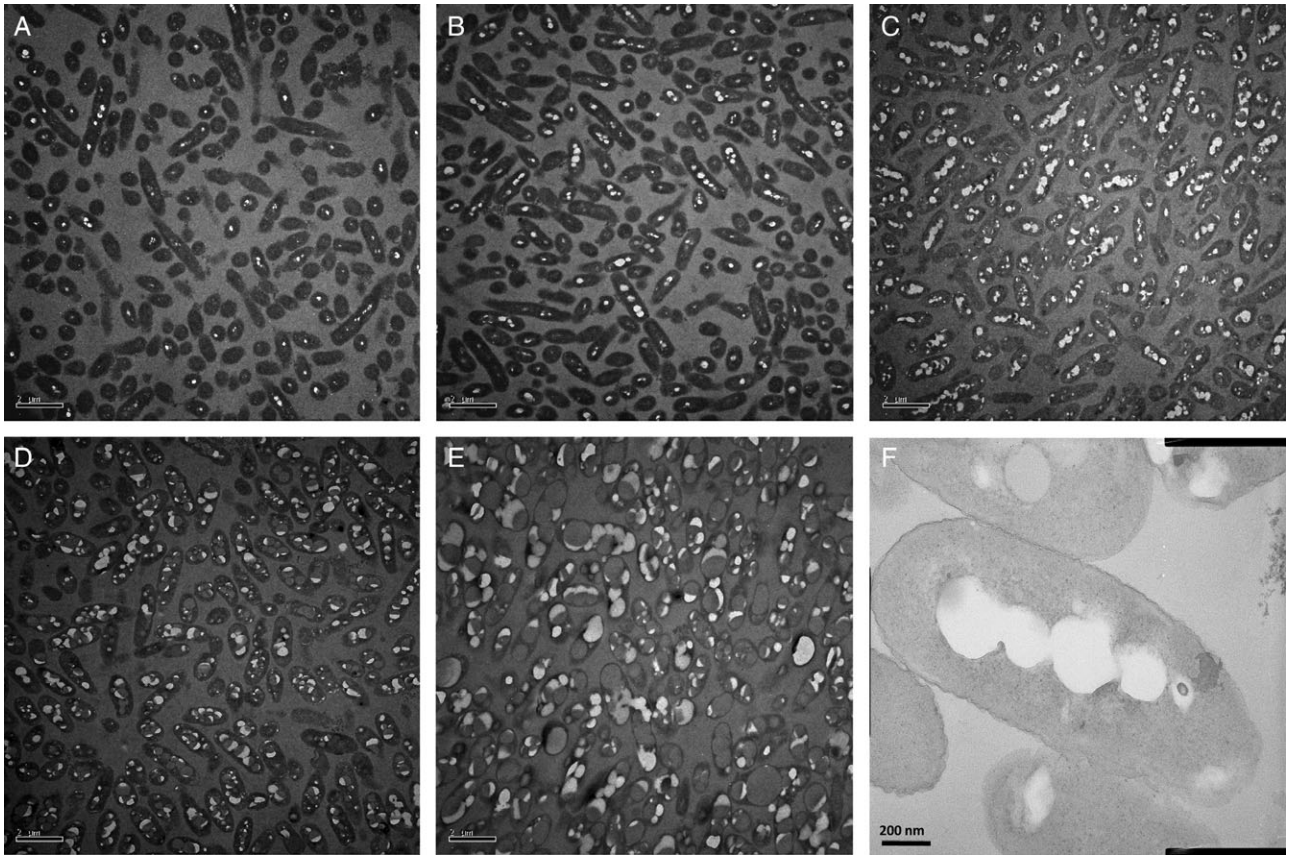

Fig. 3. TEM images of *P. putida* KT2442 cells harvested at different time points during growth in PHA production medium.
A–E. Samples were taken 0, 2, 4, 6 and 24 h after inoculating (A, B, C, D and E respectively) and processed as described in *Experimental procedures*.
F. Detail of the granule distribution of a single cell from a 4 h culture in PHA production medium.

confirmed that *P. putida* cells lacking exclusively the C-terminal half of the PhaF protein (Moldes *et al*., 2004) showed similar phenotype in terms of PHA to that of KT42F (Moldes, 2003). In addition, these results explain the reduction of the total PHA content at 24 h in the mutant strain (Fig. 2) by a dilution effect due to the presence of PHA empty cells.

DNA-binding abilities of PhaF protein and its role as transcriptional regulator

The involvement of PhaF in the *pha* transcriptional regulatory system was first demonstrated in *P. putida* GPo1 (Prieto *et al*., 1999). Disruption of the *phaF* gene led to an increased expression rate of *phaC1* gene, suggesting that PhaF acted as a negative regulator of the *pha* cluster in this strain. This function was ascribed to its C-terminal half due to the similarity observed to histone-like proteins, but there was no evidence pointing to direct binding of PhaF to the *pha* promoter regions so far.

Five different promoter regions were recently determined as part of the *pha* cluster in *P. putida* KT2442 (Fig. 1A), being P_{C1} and P_I the most active promoters of the gene cluster. P_{C1} and P_I direct the transcription of *phaC1ZC2D* and *phaIF* operons respectively (Fig. 1A) (de Eugenio *et al*., 2010a). These promoters are carbon source-dependent controlled by the PhaD regulator, which activates the transcription when fatty acids were present in the culture medium. To check whether PhaF affects the expression profile of the *pha* cluster in this model strain, the transcription rate of *phaC1, phaF* and *phaI* genes was monitored in the mutant KT42F and the wild-type strains by real-time RT-PCR. Both strains were cultured in octanoic acid or glucose as preferred or poor PHA precursors respectively (see *Experimental procedures* for details).

Transcription of *phaC1* and *phaI* genes reaches its maximum level in the wild-type strain after 8 h of culturing in the presence of octanoic acid (Fig. 7). When *phaF* was disrupted, the transcription level of *phaC1* was decreased approximately 3.5-fold respect to wild type, confirming that the lack of PhaF protein affects the transcription control of the *phaC1ZC2D* operon (Fig. 7). The expression profile of *phaI* gene was also significantly altered

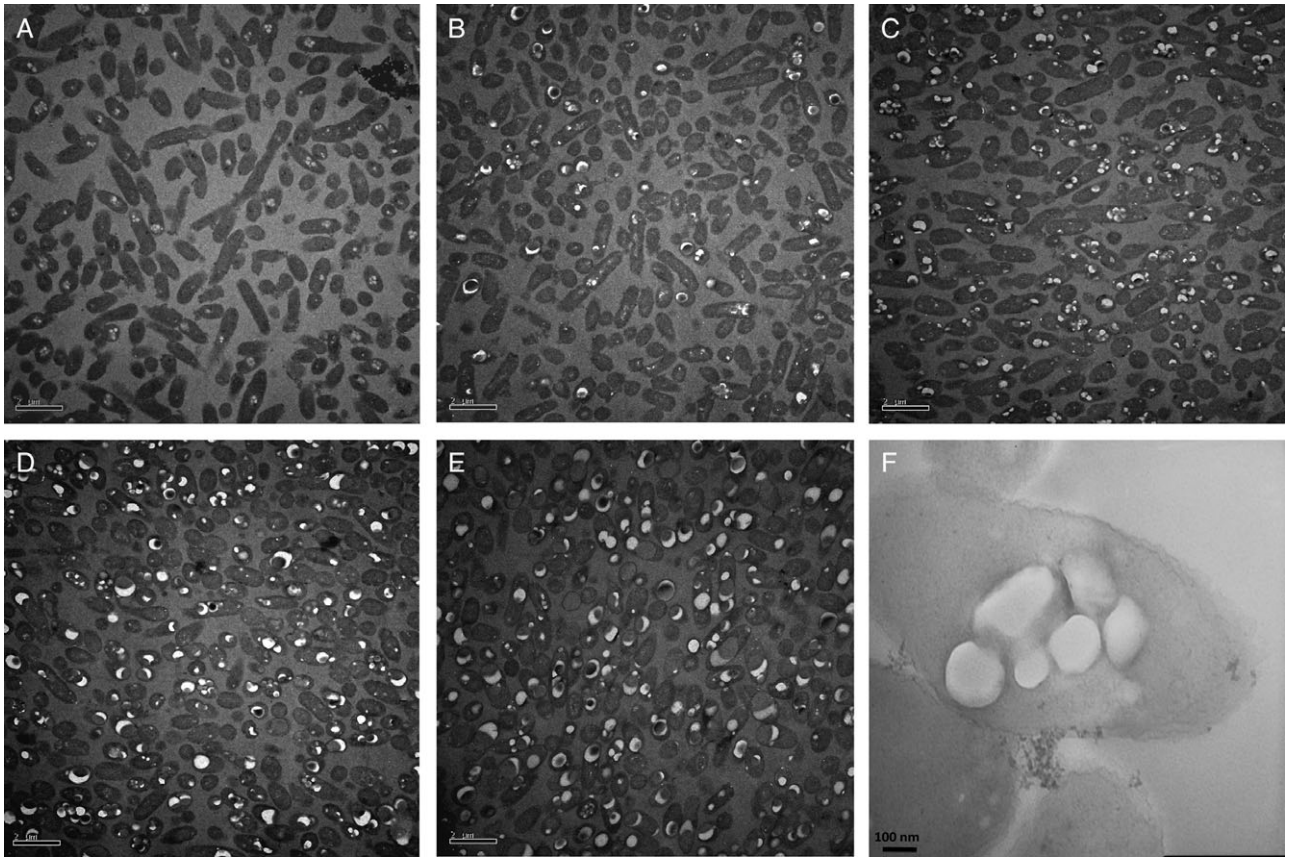

Fig. 4. TEM images of *P. putida* KT42F cells harvested at different time points during growth in PHA production medium.
A–E. Samples were taken 0, 2, 4, 6 and 24 h after the inoculum (A, B, C, D and E respectively) and processed as described in *Experimental procedures*.
F. Detail of the granule distribution of a single cell from a 4 h culture in PHA production medium.

in the mutant strain. While in the wild-type strain the maximum transcriptional level is reached in the mid-exponential phase, in the mutant strain lacking PhaF the highest transcriptional level is reached in the stationary phase (Fig. 7). The production of the PhaI phasin in the KT42F mutant strain was confirmed by SDS-PAGE analysis of the PHA granule fraction (data not shown). These results confirm that the lack of PhaF altered the transcription rate of the *pha* genes.

Taking into account the results presented above we cannot discard the possibility that PhaF, similarly to other nucleoid-associated proteins, would exert a global pleiotropic effect in other unrelated *pha* genes. The application of microarray technology has allowed us to determine the genes that are altered in the mutant strain. A total of 18 genes were significantly upregulated (2- to 9.2-fold) and 39 were downregulated (–1.9- to –27-fold) (Table S1). This result confirms that the absence of the PhaF protein affects the expression of other genes unrelated to the *pha* cluster.

The specificity of the PhaF binding to P_{C1} and P_I promoter regions was also analysed by gel retardation assays. Three different fragments were used as DNA probes: PC1 (266 bp), PI (441 bp) and PF (219 bp) covering the entire *phaC1*, *phaI* and *phaF* upstream regions respectively (Fig. 1). Purified PhaF protein was able to bind the three DNA fragments in a protein concentration-dependent manner (Fig. 8A–C). However, when 6000-fold excess amount of an unrelated DNA, such as that of salmon sperm, was added to the reaction mixture, migration of the labelled fragment was not retarded in any of the three DNA fragments tested. Similar results were obtained when unlabelled PI probe was added (Fig. 8D). These results indicated that binding of PhaF protein to DNA was not specific, i.e. it is independent of the recognition of a specific operator DNA sequence.

Binding of DNA to PhaF was also assessed by spectroscopical techniques. Near-UV circular dichroism experiments (CD) were performed with a 31-mer non-specific DNA fragment (nspDNA) that contains a sequence completely unrelated to the *pha* DNA regions. Figure 9A shows that the experimental wavelength spectrum registered for a 1:1 mixture of the whole PhaF and nspDNA differs from the theoretical sum of protein and DNA

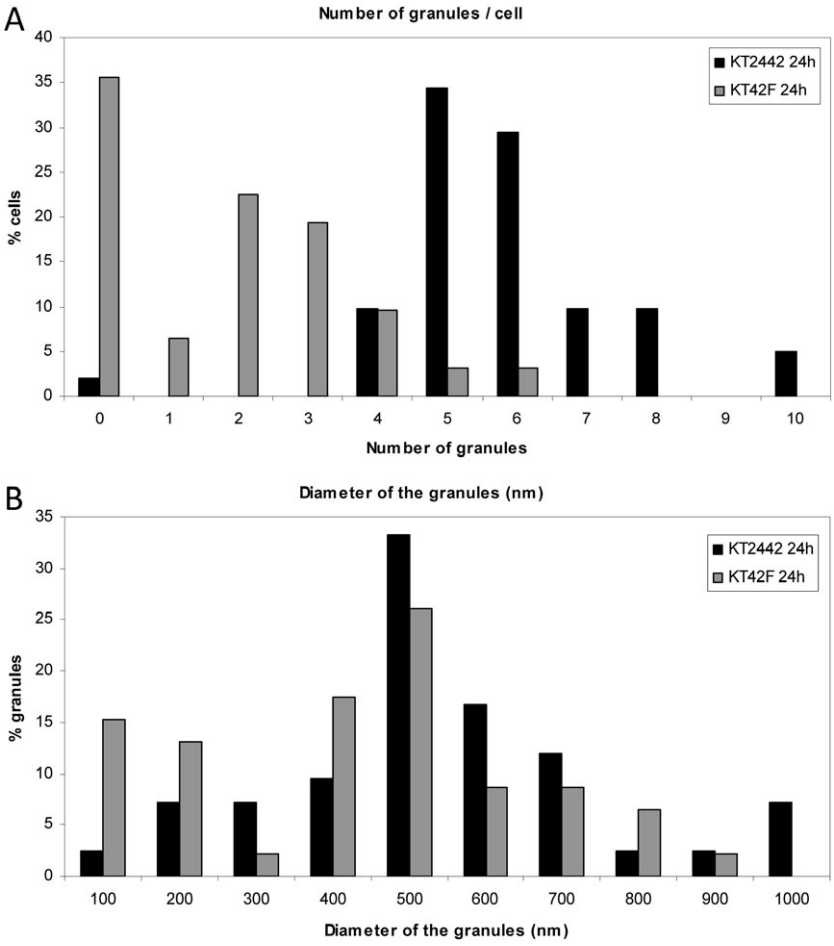

Fig. 5. Determination of granule size and number in KT2442 and KT42F strains of *P. putida*. The granule number (A) and granule size distributions (B) in KT2442 (black bars) and KT42F (grey bars) were determined by TEM images analysis as described in *Experimental procedures*.

spectra recorded separately, especially in the 260–290 nm region. This suggests the formation of a DNA–protein complex that may affect to the environment of the bases in the nucleic acid. In order to corroborate this hypothesis, the stability of the nspDNA fragment in the presence or absence of PhaF was assessed by CD-monitored thermal denaturation experiments (Fig. 9B). To exclusively check the DNA signal, we followed the ellipticity at 244 nm, a wavelength where proteins barely display an appreciable signal (Johnson, 1988). In the absence of protein, a sigmoidal transition with a melting temperature (t_m) of 54.1 ± 0.2°C was observed, whereas addition of an equimolar concentration of PhaF protein induced a significant increase in the thermal stability of the nspDNA fragment (t_m = 63.9 ± 0.2°C). To check the involvement of the PhaF C-terminal moiety in the DNA-binding properties, we expressed and purified independently this polypeptide sequence (C-PhaF) as described in *Experimental procedures*, and checked its DNA-binding capabilities by CD. Remarkably enough, the C-PhaF protein was also able to bind the nspDNA oligomer (Fig. 9), inducing a thermal stabilization of the latter comparable to that produced by full-length PhaF (t_m = 60.6 ± 0.2°C). Therefore, these results would confirm that PhaF binds *in vitro* to DNA through its C-terminal domain in a non-specific manner.

To confirm these findings *in vivo*, we have constructed a fusion protein between the reporter green fluorescent protein (GFP) and the DNA-binding domain of the protein PhaF (C-PhaF) (see *Experimental procedures*). The strains KT42-GC and KT42F-GC expressing GFP::C-PhaF fusion protein in *P. putida* KT2442 and *P. putida* KT42F, respectively, have been used to analyse the localization *in vivo* of the GFP::C-PhaF fusion protein by confocal microscopy (Fig. S1). By staining the cells with two different dyes, we have analysed the *in vivo* localization of (i) the PHA granules (Nile Red-stained), (ii) the nucleoid (DAPI-stained) and (iii) the protein GFP::C-PhaF. Our results confirm the colocalization of the fusion protein GFP::C-PhaF and nucleoid in wild-type and PhaF minus cells, independently of the presence or absence of the PHA granules. Furthermore, PHA granules produced in the wild-type cells, which contain native PhaF protein, colocalized with the nucleoid and GFP reporter. However, PHA granules produced in the KT42F mutant strain localized independently of the nucleoid and GFP reporter

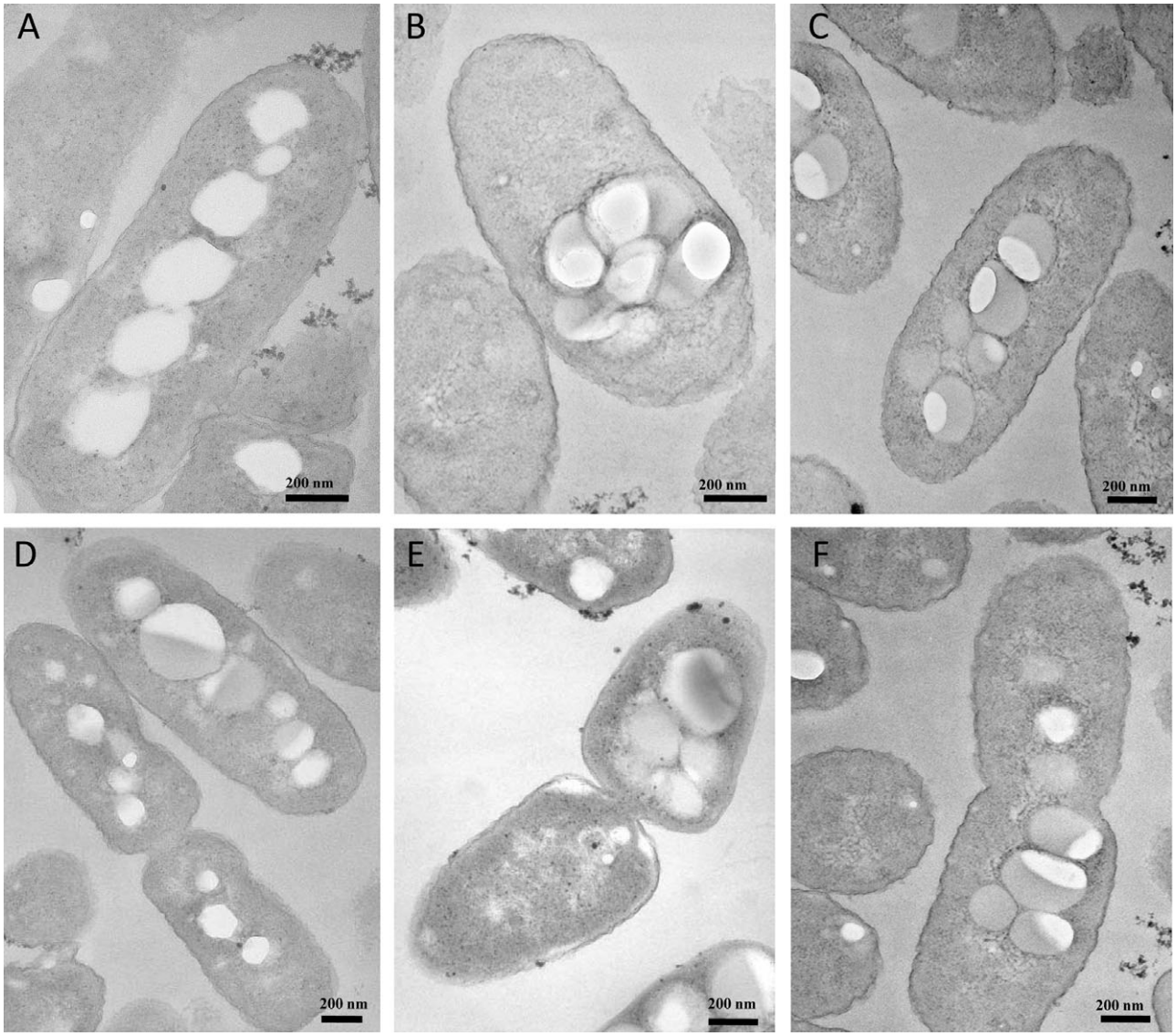

Fig. 6. Analysis of the *P. putida* KT42F complementation and PHA segregation by TEM.
A–C. Samples were taken after 4 h growth in PHA production medium. Detail of the PHA granule distribution of KT2442 (A), KT42F (B) and the complemented strain KT42F-F (C).
D–F. Segregation of PHA granules during cell division in KT2442 (D), KT42F (E) and KT42F-F (F).

system. These results provide support to the role of PhaF as nucleoid-binding protein and its function in the intracellular localization of the PHA granule.

Discussion

Phasins have been described as amphiphilic proteins which generate an interphase between the cytoplasm and the hydrophobic core of PHA granules (Steinbüchel *et al*., 1995). They are widespread among bacteria, sharing similar functions but differing in their primary structures (Grage *et al*., 2009). Generally, they consist of a hydrophobic domain which associates with the surface of the PHA granules and a hydrophilic domain which is exposed to the cytoplasm. The amphiphilic layer stabilizes the PHA granules and prevents them from coalescing (Wieczorek *et al*., 1995). Other functions proposed for phasins are: to control the number and surface of granules, to protect the host cell by contributing to coverage of the hydrophobic surface of the polymer, to prevent protein misfolding on the hydrophobic granule (Steinbüchel *et al*., 1995) or to serve as a storage source of nitrogen (McCool and Cannon, 1999). However, the role of phasins in granules formation is not understood yet (Rehm, 2006). Two models of polyhydroxybutyrate (PHB) granule formation have been described in bacteria, the micelle model and

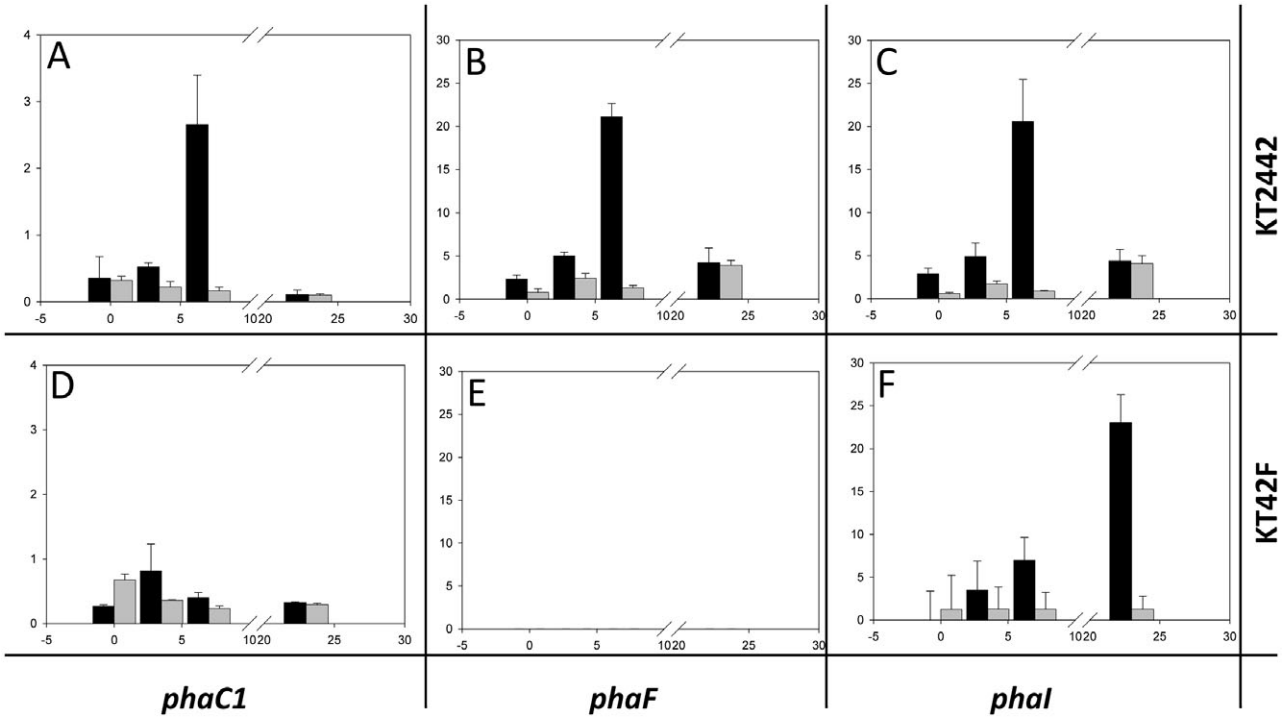

Fig. 7. Effect of the PhaF production on the expression rates of the *pha* genes. Real-time RT-PCR quantification of the *pha* genes transcription profiles throughout growth of *P. putida* KT2442 (A–C) and *P. putida* KT42F (D–F) cultured in M63 0.1 N plus 15 mM sodium octanoate (black bars) or 20 mM glucose (grey bars). An initial concentration of 5 ng of cDNA was used for quantitative RT-PCR. Error bars represent standard deviation calculated from the results of three independent experiments. *y*-axis: transcription level (cDNA ng); *x*-axis: time of culture (hours). Samples along the growth curve were taken at 0, 3.5, 7 and 23 h. The transcription of *phaC1* (A and D), *phaF* (B and E) and *phaI* (C and F) genes is depicted.

the budding model, both accounting for the stabilized location of the synthase and phasin on the surface of the granule (revised in Grage *et al*., 2009). In the micelle model, a self-assembly process is initiated resulting in the formation of insoluble cytoplasmic inclusions with a phospholipid monolayer which contains covalently attached polyester synthases at the surface. In the budding model, the hydrophobic synthase binds to the inner face of the plasma membrane and buds from this membrane, leading to a granule surface covered with a lipid monolayer and phasins. However, TEM studies of granule formation and degradation in *Cupriavidus necator* H16 (formerly *Ralstonia eutropha* H16) revealed dark-stained elements ringed by small granules at early stages of PHB production. These structures named 'mediation elements' were located near the centre of cells or along a longitudinal strip in the centre of the cells (Tian *et al*., 2005). These results were at odds with the micelle and membrane budding models, and led to an alternative model for granule formation, in which granules are localized and the new 'mediation elements' function as scaffolds for the granule initiation sites. The fate of granules during cell division, that is, whether they are equally distributed between daughter cells, is not known (Tian *et al*., 2005).

We have explored the physiological role of the nucleoid-associated phasin PhaF from the prototype microorganism *P. putida* KT2442. One of the peculiarities of this protein is its modular organization in a PHA granule-binding domain (located at the N-terminus) and an AKP-rich domain (located at the C-terminus). In fact, we had previously demonstrated the abilities of PhaF from *P. putida* GPo1 for binding to PHA granule (phasin-like activity), and as transcriptional regulator, suggesting a putative DNA-binding activity (Prieto *et al*., 1999; Moldes *et al*., 2004). This C-terminal domain from the PhaF protein with a DNA-binding function nucleoid-associated is unique among phasins. In this sense, the identified phasins from *C. necator* H16 (PhaP1, PhaP2, PhaP3 and PhaP4) display an alanine-rich C-terminal region showing a very high isoelectric point (Neumann *et al*., 2008). Nevertheless, further investigations are needed to exclude that this positive charge might participate in the interaction with the 'mediation elements' or the latter might be simply the nucleoid of the cell.

This work demonstrates that PhaF plays a crucial role in granule localization and distribution, since the lack of this protein unbalance granule segregation during cell division (Fig. 6). Similar system of localization of

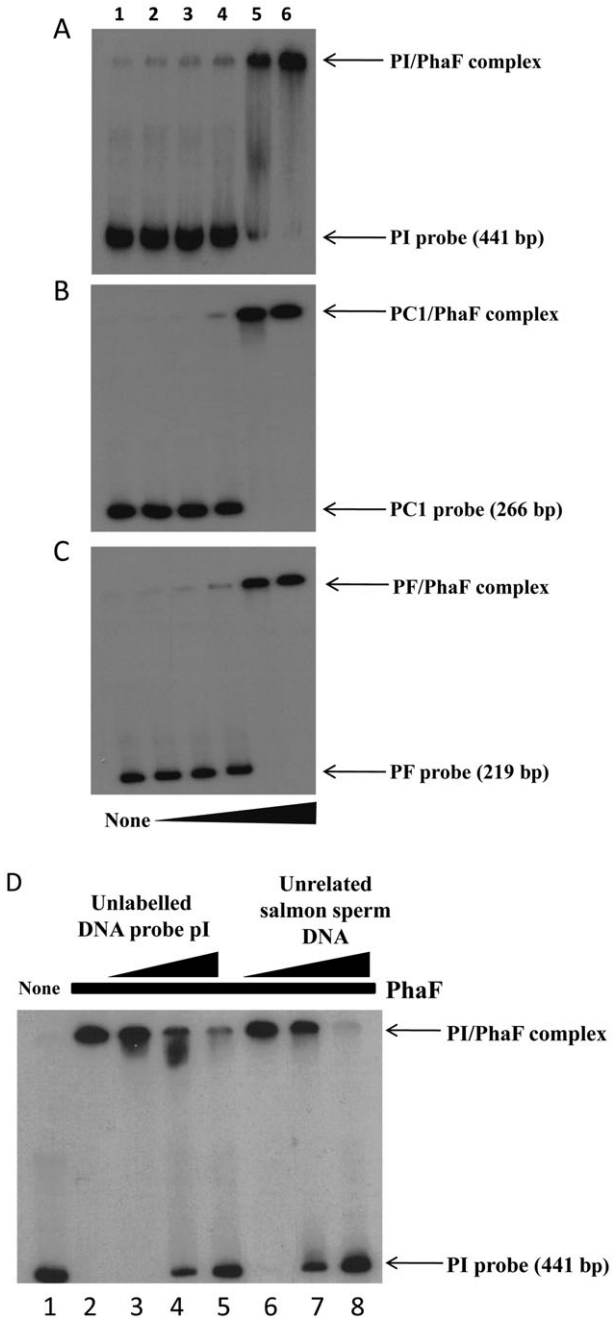

Fig. 8. Gel retardation analyses of PhaF binding to the P_I, P_{C1} and P_F promoter regions.
A–C. The DNA probes used [PI (A), PC1 (B) and PF (C)] are indicated schematically on the right of the figure. PhaF protein purification and gel retardation analyses were performed as described in *Experimental procedures*. Lanes 2–6, contained increasing concentrations (30, 50, 100, 200 and 500 nM) of PhaF protein. Lane 1 contained no protein. The DNA–PhaF complexes are indicated.
D. PhaF-binding competition analysis to P_I promoter with unlabelled DNA-specific probe (lanes 3–5) and unrelated salmon sperm DNA (lanes 6–8). Gel retardation was performed in the presence of 300 nM PhaF. Lane 1 contains no PhaF protein. Lane 2 is a control containing no unlabelled specific probe.

organelles as needle array inside prokaryotic cells has been observed for the intracellular organelles magnetosomes from *Magnetospirilum gryphiswaldense* (Komeili *et al*., 2006). They are assembled into a regular chain in order to achieve the maximum magnetic moment, against the physical tendency of magnetosome agglomeration. In this system, the protein responsible for this alignment is MamJ which has a high content of acidic amino acids and a repeated domain structure, which appears to interact with a linear cytoskeleton-like structure composed by MamK (actin-like protein) that directs the assembly and localization of the prokaryotic organelles (Scheffel *et al*., 2006). *P. putida* KT2442 (Nelson *et al*., 2002) posses members of all cytoskeletal systems described in bacteria (revised in Gitai *et al*., 2005; Gerdes *et al*., 2010) like the tubulin homologous FtsZ (annotated as PP_1342 in the chromosome); ParAB (PP_0001-2) and MinCDE (PP_1732-34) systems, where ParA and MinD are similar variant P loop ATPases that form cytoskeletal-like filaments on DNA and membranes, respectively, to solve different problems (DNA segregation and septum placement) by analogous molecular mechanisms; actin homologue MreB (PP_0934), similar to the actin-like protein MamK, which forms a helix essential for maintenance of cell shape, and it has been recently hypothesized to act as a scaffold for transporting proteins to different locations throughout the bacterial cell (Kimberly and Gitai, 2010). Our work revealed PhaF as central player in the machine to control PHA granule segregation and localization in the cell. Moreover, whether or not *P. putida* KT2442 cytoskeletal proteins facilitate the needle array structure by direct or indirect interaction with PhaF is still an open question and at this point, the precise mechanisms by which PHA granules are positioned by PhaF remains elusive. Since PhaF shows a unique ability for binding at least two ligands, the PHA granules and the nucleoid, our work provides support to consider that the PhaF function localizing and segregating the PHA granules implies new mechanisms different from that of described for magnetosomes (MamK/MamJ) or DNA segregation in bacteria (ParA-like mechanism). Taking into account the unspecific DNA-binding abilities of the C-terminal part of PhaF, we cannot discard that the bacterial chromosome could play a role as granule carrier during the division process. In this sense, previous studies have determined the cellular position of different chromosomal sites demonstrating that they were positioned along the long axis of the cell in a linearly ordered fashion from the origin to the terminus (Teleman *et al*., 1998; Niki *et al*., 2000; Viollier *et al*., 2004).

The unspecific PhaF–DNA interaction validates the classification of this phasin as nucleoid-associated protein and raises further questions about the physiological roles of PhaF in *P. putida*. Eukaryotic H1 histones are also

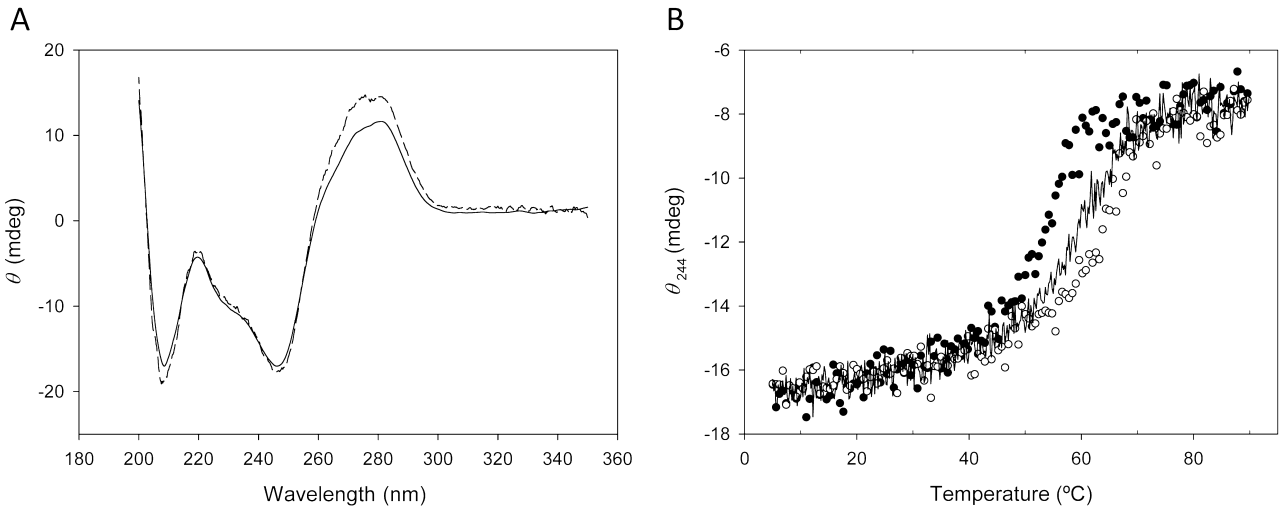

Fig. 9. Binding of PhaF and C-PhaF to DNA monitored by CD.
A. Wavelength spectra of a solution containing 9 μM PhaF and 9 μM nspDNA (solid line), and theoretical spectra obtained from the arithmetic sum of spectra recorded for 9 μM PhaF and 9 μM nspDNA separately (dashed line).
B. Thermal stability of 9 μM nspDNA (black circle), 9 μM nspDNA plus 9 μM PhaF (white circles) and 9 μM nspDNA plus 9 μM C-PhaF (solid line).

called linker histones because they are chromatin-associated proteins that bind to the exterior of nucleosomes and dramatically stabilize the highly condensed states of chromatin fibres (Zlatanova *et al*., 2000). In eukaryotic organisms, there is evidence that linker histones are also involved in transcriptional regulation by determining the accessibility of the nucleosomal DNA to the transcriptional machinery (Zlatanova *et al*., 2000). Furthermore, it has been demonstrated that histones of the H1 family provide the DNA compaction required by the changing physiological needs of the cell during the different stages of cell cycle (Kasinsky *et al*., 2001). We have undoubtedly demonstrated that the lack of PhaF protein in *P. putida* affects transcription rate of *pha* cluster. Moreover, the transcriptomic analysis carried out in the strain KT42F suggested that the expressions of other genes unrelated to PHA metabolism were also modified in this strain, but the mechanism involved in this global effect is still unclear and pleiotropic effects related to the existence of two populations in terms of PHA content cannot be excluded. Even more, PhaF might contribute to the chromosomal DNA overcondensation needed when the cells contained more than 50% of PHA of CDW in the cytoplasm.

Examples of bi-functional proteins containing the AKP-rich domain are found in eukaryotic organisms, such as the ribosomal proteins L22 and L23a of *Drosophila melanogaster* (Koyama *et al*., 1999), and in the prokaryotic organisms like AlgP from *P. aeruginosa* (Deretic and Konyecsni, 1990) and the putative DnaK suppressor from *Stenotrophomonas* sp. It is also worth to mention the cases of the translation factor IF-2 from Actinobacteria which contains an AKP-rich region in its N-terminal domain that is involved in translation initiation and binds to the ribosome by interacting with the initiator tRNA (Caserta *et al*., 2006). Also, the Hc1 and Hc2 proteins from *Chlamydia trachomatis* play a role in the chromosome condensation regulating the stage-specific differentiation during the life cycle (Kaul *et al*., 1996) and BpH1 and BpH2 proteins from *Bordetella pertussis,* which are known to condense the DNA and protect it from digestion with DNase I *in vitro*, could be involved in transcriptional regulation (Goyard, 1996).

Summing up, we have described here a new and unexpected role for the PhaF phasin of *P. putida* KT2442 involved in the balanced distribution of the PHA reserve granules between daughter cells during cell division. This ability has been ascribed to the particular composition of its C-terminal domain which mimics nucleoid-associated proteins, and confers the protein an unspecific DNA-binding capacity. Therefore, the distribution of reserve materials between the two daughter cells appears to be associated to the co-ordinated segregation of chromosomes, which might act as granule carriers through PhaF interactions. These findings lead arguments to an alternative model for PHA granule formation in bacteria, open a more complex view of the bacterial organelles segregation and transcriptional regulation related to PHA metabolism, and demonstrated a new role for phasins within the PHA apparatus that could be critical for cell survival under stress conditions.

Experimental procedures

Bacterial strains, plasmids, media and growth conditions

The *P. putida* strain KT2442, a derivative strain of the parental strain KT2440 whose complete nucleotide sequence of the genome is accessible in the data bank (Nelson *et al.*, 2002), was used throughout this study. *Escherichia coli* DH10B (Invitrogen) and *E. coli* BL21(DE3) (harbouring the T7 RNA polymerase gene under control of the *lacUV5* promoter) were used as hosts for gene cloning and overexpression respectively. Plasmid pET-29a(+) (Novagen) is an *ori*ColE1 vector that confers kanamycin resistance and allows gene cloning and expression under the control of the T7 promoter. *E. coli* cells were grown with aeration at 37°C in Luria–Bertani medium (Sambrook and Russell, 2001) containing, where appropriate, 50 μg ml^{-1} kanamycin. *P. putida* KT2442 cells were cultivated with aeration at 30°C. For optimal PHA production, a pre-culture of the *P. putida* strains was cultivated overnight in LB medium, washed and inoculated at 0.3 OD_{600} in 0.1 N M63, which is a nitrogen-limited minimal medium in the presence of 15 mM octanoic acid as carbon source (de Eugenio *et al.*, 2010b). The appropriate selection antibiotics, kanamycin (50 μg ml^{-1}), gentamicin (5 μg ml^{-1}) or rifampicin (50 μg ml^{-1}), were added when needed.

Molecular biology techniques

Standard molecular biology techniques were performed as previously described (Sambrook and Russell, 2001). PCR products were purified with the High Pure plasmid isolation kit (Roche Applied Science). DNA fragments were purified with Gene-Clean Turbo (Q-BIO-gene). Genomic DNA from *P. putida* KT2442 was isolated with the Genomic Prep Cells and Tissue DNA Isolation kit (Amersham Biosciences). All cloned inserts and DNA fragments were confirmed by DNA sequencing with fluorescently labelled dideoxynucleotide terminators and AmpliTaq FS DNA polymerase (Applied Biosystems) in an ABI Prism 377 automated DNA sequencer (Applied Biosystems). Transformation of *E. coli* cells was carried out using the RbCl method (Sambrook and Russell, 2001).

Construction of a PhaF null mutant of P. putida *KT2442*

The *phaF* gene was inactivated by marker exchange as described previously using the mobilizable suicide plasmid pKNG101 (Kaniga *et al.*, 1991). The deletion of *phaF* gene was engineered with the DNA fragments DmutF and ImutF of 575 bp and 402 bp, respectively, generated by PCR using the primer pairs D5mutF 5′-CGGGATCCCAACGAACTCGGC ATCAGC-3′ and D3MutF 5′-CGGAATTCCAACACTACATC TCCAGCAG-3′ for DmutF, and I5mutF 5′-CGGAATTCGCCA GCCATCCTGCTCTCC-3′ and I3mutF 5′-TCCCCCGGGC TGGACACGCTTGGCGAGG-3′ for ImutF. These two fragments were digested with the appropriate restriction enzymes and ligated using T4 ligase resulting in a single 977 bp fragment carrying a deletion of the *phaF* gene which was cloned into the unique BamHI and SmaI sites of pKNG101 to yield pKNGFdel. Plasmid pKNGFdel was used to deliver the *phaF* mutation to the host chromosome via homologous recombination. Biparental mating was performed following protocols described by de Lorenzo and Timmis (1994), using *E. coli* SM10λpir (pKNGFdel) as donor strain and *P. putida* KT2442 as recipient strain. For conjugation, 100 μl of overnight cultures of donor and recipient strains were mixed in 5 ml of 10 mM $MgSO_4$ and collected on a Millipore filter which was subsequently placed on an LB agar plate and incubated overnight at 30°C. After incubation, the cells were resuspended in 5 ml of 10 mM $MgSO_4$ and plated on M63 selective plates supplemented with 5% sucrose as described previously (Kaniga *et al.*, 1991). Transconjugants (Suc^R, Sm^S) were isolated. The second cross-over event was confirmed by PCR using primers D5MutF and I3MutF. The resultant mutant strain was denoted KT42F.

Flow cytometry

Cells were harvested and washed twice with distilled water and resuspended in water to a final OD_{600} of 0.2 for staining with Nile Red. A Nile Red stock solution was made by dissolving the dye to a concentration of 1 mg ml^{-1} in dimethyl sulphoxide (DMSO). Three microlitres of stock solution were added to 1 ml of cell suspension. The mixture was incubated in the dark for 15 min and analysed by flow cytometry (flow cytometer Coulter EPICS XL). *P. putida* KT42C1 minus strain (a *phaC1* mutant which produces < 1% CDW PHA) (de Eugenio *et al.*, 2010b) was used as negative control. A calibration curve for the quantification of the PHA content using flow cytometry was made comparing the fluorescence intensity and PHA content analysed by gas chromatography throughout the growth curve in *P. putida* KT2442 (data not shown). The relation between both parameters was fitted to the equation $y = 30.874\ \mathrm{Ln}(x) + 38.11$ with a $R^2 = 0.9984$. This equation has been used to translate the cytometry fluorescence intensity data into PHA values.

Complementation of P. putida *KT42F*

Plasmid pPF61, harbouring the *phaF* gene from *P. putida* GPo1 under the control of the *Ptrc* promoter (Prieto *et al.*, 1999), was introduced into *P. putida* KT42F chromosome by triparental mating. The resulting strain called KT42F-F was cultivated in PHA production medium in the presence of 5 mM isopropyl-1-thio-β-D-galactopyranoside (IPTG) as described (Prieto *et al.*, 1999).

Transmission electron microscopy

Cells were harvested, washed twice in PBS and fixed in 5% (w/v) glutaraldehyde in the same solution. Afterwards, cells were suspended in 2.5% (w/v) OsO_4 for 1 h, gradually dehydrated in ethanol [30%, 50%, 70%, 90% and 100% (v/v); 30 min each] and propylene oxide (1 h), embedded in Epon 812 resin. Ultrathin sections (thickness 70 nm) were cut with a microtome using a Diatome diamond knife. The sections were picked up with 400 mesh cupper grids coated with a layer of carbon and subsequently observed in a Jeol-1230 electron microscope (JeolLtd., Akishima, Japan).

To determine the size of PHA granules from the micrographs, 50 cells of the wild type and of the mutant were

selected, in which the PHA granule diameter was measured. We analysed 100 granules of the wild type and 100 of the mutant. Only granules with sharp boundaries were selected. The number of PHA granules per cell was determined only from cells which were fully visible in the electron micrographs.

Construction of P. putida *strains expressing a cassette consisting in a fusion gene* GFP *and C- terminal domain of PhaF*

The GFP::C-PhaF fusion was obtained by amplification of two DNA fragments. GFP cassette was amplified from plasmid pGreenTIR (Miller and Lindow, 1997) with GFP-F 5′-GGGAATTCTGATTAACTTTATAAGGAGGAAAAACAT-3′ (an engineered EcoRI restriction site is underlined) and GFP-RBamHI 5′-CGGGATCCTTTGTATAGTTCATCCATGCCAT-3′ (an engineered BamHI restriction site is underlined) oligonucleotides. After digestion with the corresponding restriction endonucleases, the GFP cassette was cloned into pUC18Not plasmid yelding pUC18NotGFP. *phaF* C-terminal domain was PCR amplified using C-termF (GFP) 5′-CGGGATCCTCGCGCGCTGCAGCAAC-3′ (an engineered BamHI restriction site is underlined) and C-termR (GFP) 5′-GCCAAGCTTCAGATCAGGGTACCGGTGCC-3′ (an engineered HindIII restriction site is underlined) oligonucleotides from genomic DNA of *P. putida* KT2442. Obtained PCR product was digested and cloned into pGEM-T plasmid. The fragment obtained after digestion with HindIII and BamHI was cloned into pUC18NotGFP plasmid. The resulting hybrid plasmid pUC18NotGFP-Cterm was transformed into *E. coli* strain DH10B. Construction was confirmed by sequencing using an ABI Prism 3730 DNA Sequencer. The GFP::C-PhaF fusion was cloned from pUC18NotGFP-Cterm plasmid into pCNB5 vector as NotI fragment. Constructed plasmid pCNB5-GFP-Cterm was introduced into the *P. putida* KT2442 and *P. putida* KT42F chromosomes by triparental mating yielding KT42-GC and KT42F-GC respectively. Conjugates were isolated after plating on M63 0.1 N selective plates supplemented with 0.2% citrate and kanamycin. Afterwards colonies were picked in LB plates and LB plates with IPTG and selected with a fluorescent magnifying lamp.

In vivo *localization of the C-terminal domain of PhaF by fluorescence microscopy*

Pseudomonas putida KT42-GC and KT42F-GC strains were cultivated overnight in LB medium. Then, cells were washed and inoculated at 0.3 OD_{600} in 0.1 N M63. Cultures were induced with 2 mM IPTG in the exponential phase of growth to induce the production of the GFP::C-PhaF fusion protein. Nucleoids staining was performed by incubation with 2 μg ml^{-1} DAPI for 15 min while the PHA granules were visualized after staining with 1 μg ml^{-1} Nile Red for 15 min. Then cells were fixed with 4% paraformaldehyde at room temperature for 1 h, washed tree times with PBS and visualized by confocal microscopy Laser Confocal espectral (CLSM) Leica TCS SP2-AOBS.

Real-time RT-PCR assay

Total RNA was extracted from *P. putida* KT2442 and *P. putida* KT42F strains. Cells were inoculated at 0.3 OD_{600} in 0.1 N M63 medium with 15 mM octanoate or 10 mM glucose as carbon sources. Cells were harvested throughout the growth curve and stored at –20°C. Pellets were thawed and cells lysed in TE buffer (10 mM Tris-HCl pH 7.5, 1 mM EDTA) containing 5 mg ml^{-1} lysozyme by a series of freeze/unfreeze cycles. RNAs were extracted using the RNeasy mini Kit (Qiagen), including a DNase I treatment according to the manufacturer's instructions, precipitated with ethanol, washed and resuspended in 40 μl of RNase-free water. The concentration and purity of the RNA samples were measured by ND1000 Spectrophotometer (Nanodrop Technologies). Synthesis of total cDNA was carried out with 20 μl of reverse transcription reactions containing 1 μg of RNA, 0.5 mM dNTPs, 200 U of SuperScript II Reverse Transcriptase (Invitrogen) and 5 μM random hexamers as primers, in the buffer recommended by the manufacturer. Samples were initially heated at 65°C for 5 min and then were incubated at 42°C for 1 h, terminated by incubation at 70°C for 15 min. The cDNA obtained was purified using Geneclean Turbo Kit (MP Biomedicals) and the concentration was determined by a ND1000 Spectrophotometer (Nanodrop Technologies). For the analysis of the transcript levels target cDNAs (5 ng) and reference samples were amplified three times in separate PCR reactions using 0.2 μM of primers C1RT5′ (5′-CTGGGCACCAGCGAAGGCG-3′) and C1RT3′ (5′-GTAATCGACAGCACCGCGTC-3′) for *phaC1,* F-RTf (5′-GTCATGTTTAGACGGAATACCCAG-3′) and F-RTr (5′-GCGGCCAACCACCAGCTTG-3′) for *phaF* and I-RTf (5′-GCACCGGTCAGCTTCTCGATC-3′) and I-RTr (5′-GGAGCGAACTTGAAGAAGCC-3′) for *phaI* by iQ5 Multicolor Real-Time PCR Detection System (Bio-Rad). Real-time PCR was performed using SYBR Green technology in an ABI Prism 7000 Sequence Detection System (Applied Biosystems). Samples were initially denatured by heating at 95°C for 4 min, followed by 30 cycles of amplification (95°C, 1 min; test annealing temperature, 65°C, 1 min; elongation and signal acquisition, 72°C, 30 s). For relative quantification of the fluorescence values, a calibration curve was made using dilution series from $5 \cdot 10^{-7}$ to 5 ng of *P. putida* KT2442 genomic DNA sample.

Hybridization and processing of DNA microarrays

RNA for microarray analyses was obtained from three independent cultures grown under identical conditions. Precultures of the *P. putida* strains were cultivated overnight in LB medium, washed, inoculated at 0.3 OD_{600} in PHA production medium and grown during 8 h.

Aliquots of 50 ml were harvested by centrifugation at 4°C and frozen at –20°C. The cell pellet was resuspended in 1 ml of TriPure Isolation Reagent (Tri Reagent LS, Molecular Research Center) and incubated at room temperature for 5 min, after which cell lysis was complete. The solution was centrifuged in a microfuge at 12 000 r.p.m. for 10 min at 4°C and the pellet was discarded. Two hundred microlitres of chloroform was added to the supernatant and the mixture was vigorously shaken for 15 s. After 15 min at room temperature, the mixture was centrifuged (12 000 r.p.m., 15 min, 4°C) and the aqueous phase was recovered. Five hundred microlitres of isopropanol was added and, after 10 min at room temperature, the sample was centrifuged at 12 000 r.p.m. for 10 min at 4°C. The pellet was washed with 70% (v/v)

ethanol, dried and resuspended in 300 µl of H_2O. DNase I (2 µl, 10 units μl^{-1}) was added and the mixture incubated at 37°C for 2 h. After extracting the sample two to three times with acid phenol, the nucleic acids were recovered by precipitation with sodium acetate and ethanol. The pellet was washed with 70% (v/v) ethanol, dried and resuspended in 100 µl of H_2O. After discarding the presence of contaminating DNA by polymerase chain reaction (PCR), the samples were purified by using RNeasy columns (Qiagen), which helped to eliminate the 5S rRNA. RNA integrity was checked with a capillary electrophoresis system (Agilent 2100 Bioanalyzer).

cDNA was obtained from RNA preparations of the control and test strains (KT2442 and KT42F respectively), fluorescently labelled with either Cy3 or Cy5, mixed, and used to hybridize the DNA microarray as reported previously (Yuste *et al*., 2006). Four microarrays corresponding to independent experiments (biological replicas) were used and statistically analysed as described before (Yuste *et al*., 2006) using the LIMMA software package (Smyth, 2004). The results for each replica (mean intensity for each spot) were normalized within each array using the lowest intensity-depend normalization method (Yang *et al*., 2002) and between arrays using the scale method (Yang *et al*., 2002). Differential expression was calculated using linear models and empirical Bayes moderated *t*-statistics (Smyth and Speed, 2003; Smyth, 2004). The probability values obtained (*P*-values) were adjusted for multiple testing to control the false discovery rate (Benjamini and Hochberg, 1995). Genes were considered differentially expressed when they fulfilled the filter parameters of expression ratio ≥ 1.9 and FDR ≤ 0.1. The replica with lowest adjusted *P*-value was chosen for each gene. Data have been deposited at http://www.ebi.ac.uk/arrayexpress/.

Gel retardation assays

For the labelling of the probes in competition gel retardation assays DNA fragments of 266, 451 and 219 bp containing the P_{C1}, P_I and P_F promoters (de Eugenio *et al*., 2010a) were amplified by PCR using 100 ng of *P. putida* KT2442 genomic DNA as template and a combination of one unlabelled primer and the second primer 5′ end-labelled with phage T4 polynucleotide kinase [γ-^{32}P]-ATP (3000 Ci $mmol^{-1}$). The primers used were PI5 (5′-CCGGAATTCGCCAGAAAATGCCTGAG AAGCTC-3′) and the labelled primer PI3 (5′-CGCGGATC CATGCTGTGTACCTCATGCTC-3′), for the PI DNA fragment containing P_I promoter, PC13 (5′-CGGGGATCCATCTACG ACGCTCCGTTGT-3′) and the labelled primer PC15 (5′-TTTGAATTCGGCCTGCGGGGTTTAGAG-3′) for the PC1 DNA fragment containing P_{C1} promoter and pF5 (5′-CCGGAATTCCCAGCTTGACGAAGTCGGTGA-3′) and the labelled primer pF3 (5′-CGCGGATCCATCCTGCTCTCCT TATGGTTTGTG-3′) for the DNA fragment PF containing P_F promoter. The reaction mixtures contained 9 µl of 20 mM Tris-HCl pH 7.5, 50 mM KCl, 500 µg ml^{-1} BSA, 1 nM DNA probe and purified PhaF in a 20 µl final volume (see below). After incubation for 5 min at room temperature, mixtures were fractionated by electrophoresis in 5% polyacrylamide gels buffered with 0.5× TBE (45 mM Tris-borate, 1 mM EDTA). The gels were dried onto Whatman 3MM paper and exposed to Hyperfilm MP (Amersham Pharmacia Biotech).

Overproduction and purification of PhaF protein

The *phaF* gene was PCR amplified from *P. putida* KT2442 genomic DNA using the oligonucleotides PhaF F (5′-GG AATTCCAT**ATG**GCTGGCAAGAAGAACACC-3′; the *phaF* start codon is indicated in boldface letter, and an engineered NdeI restriction site is underlined) and C-term BamHI (5′-CGGGATCCTCAGATCAGGGTAACCGGTGCC-3′; an engineered BamHI restriction site is underlined). The resulting 808 bp DNA fragment was ligated as a NdeI/BamHI DNA fragment into the NdeI/BamHI double-digested pET-29a(+) plasmid, giving rise to plasmid pETPhaF (6.2 kb) that express the *phaF* gene under the control of the T7*lac* promoter and the ribosome binding site from the pET-29a(+) plasmid. *E. coli* BL21(DE3) cells harbouring plasmid pETPhaF were grown until the cultures (1 l) reached 0.6 OD_{600}. Overexpression of the cloned gene was then induced during 3 h by the addition of 0.2 mM IPTG. Cells were harvested at 4°C, resuspended in 50 ml of 20 mM sodium phosphate buffer, pH 7.0 plus 100 mM NaCl, disrupted by sonication (Branson 250 instrument) and centrifuged again at 4°C (10 000 *g*).

Inclusion bodies containing denatured PhaF were redissolved in 25 ml of 8 M urea followed by centrifugation for 15 min at 4°C (10 000 *g*). PhaF refolding was achieved by drop-to-drop addition to 250 ml of 20 mM sodium phosphate buffer, pH 7.0. The sample was centrifuged for 15 min at 4°C (10 000 *g*). Ammonium sulphate was then slowly added to the supernatant to a final concentration of 1.7 M, centrifuged again at 4°C (10 000 *g*) and the supernatant was applied onto a butyl sepharose 4 Fast Flow column (GE Healthcare) (10 × 1 cm) previously equilibrated in the same buffer as the sample. Column was extensively washed with 0.75 M ammonium sulphate, and finally the PhaF protein was eluted with 20 mM sodium phosphate buffer, pH 7.0 with a yield of around 20 mg per litre of culture and a purity of more than 95% as assessed by SDS-PAGE. Protein concentration was determined spectrophotometrically using a molar absorption coefficient at 280 nm (ε_{280}) of 19 071 M cm^{-1}, calculated according to Fasman (1976). Purified samples were dialysed against 10 mM ammonium hydrogencarbonate, lyophilized and stored at −80°C in aliquots until needed.

Overproduction and purification of the C-terminal domain of PhaF (C-PhaF protein)

The *phaF* C-terminal domain was PCR amplified from *P. putida* KT2442 genomic DNA using oligonucleotides C-term NdeI (5′-GGATTCCATATGTCGCGCGCTGCAGCAA CCAAG-3′; an engineered NdeI restriction site is underlined) and C-term BamHI (see sequence above). The resulting 383 bp DNA fragment was ligated as a NdeI/BamHI DNA fragment into the NdeI/BamHI double-digested pET-29a(+) plasmid, giving rise to plasmid pETCterm (5.7 kb) that express the *phaF* C-terminal encoding domain under the control of the T7*lac* promoter and the ribosome binding site from the pET-29a(+) plasmid. *E. coli* BL21(DE3) cells harbouring plasmid pETCterm were grown at 37°C until the cultures (1 l) reached an OD_{600} of 0.6. Overexpression of the cloned gene was then induced during 3 h by the addition of 0.2 mM isopropyl-1-thio-β-D-galactopyranoside. Cells were harvested at 4°C, resuspended in 50 ml of 50 mM Tris-HCl

buffer, pH 8.8 plus 10 mM $MgCl_2$, disrupted by sonication (Branson 250 instrument), incubated with DNase I (25 μg ml^{-1}) 15 min at room temperature and centrifuged again at 4°C (10 000 *g*). The supernatant was applied onto an Econo-Pac CM cartridge 5 × 1 (Bio-Rad) previously equilibrated in the same buffer as the sample. Column was extensively washed with the same buffer as above, and then subjected to a second wash with 0.7 M Tris-HCl buffer, pH 8.8. Finally the C-PhaF protein was eluted with 0.7 M Tris-HCl buffer, pH 8.8 plus 4 M NaCl with a yield of 30 mg per litre of culture and a purity > 95% as checked by SDS-PAGE. Since C-PhaF lacks any aromatic residues and has a peculiarly charged amino acid composition that might be inadequate for usual colorimetric methods, protein concentration was determined by peptidic bond absorbance at 205 nm according to Scopes (1974).

Circular dichroism spectroscopy

Near-UV circular dichroism (CD) experiments were carried out in a Jasco J-810 spectropolarimeter equipped with a Peltier PTC-423S system. Isothermal wavelength spectra were acquired at a scan speed 50 nm min^{-1} with a response time of 2 s and averaged over at least six scans at 20°C. For DNA-binding experiments, an unspecific DNA fragment (nspDNA) was prepared from hybridization of oligonucleotides 5′-AATTCACAGTAAAACCAGATGGCTTGATTAC-3′ and its complementary strand (Invitrogen), to a final stock concentration of 0.5 mg ml^{-1}. Protein and nspDNA concentration was 9 μM and the cuvette path length was 1 cm. Raw ellipticities (θ) are expressed in milidegrees. For the CD-monitored thermal denaturation experiments, the sample was layered with mineral oil to avoid evaporation, and the heating rate was set to 60°C h^{-1}. Melting temperatures (t_m) were calculated upon fitting the thermal denaturation curves to a simple sigmoidal equation with sloping baselines, using the SIGMAPLOT 10.0 utilities (Systat Software).

Acknowledgements

We are greatly indebted to Dr Pedro Lastres and Dr Jose Yuste for helpful discussions and technical support in flow cytometry analyses. We also appreciate the technical support of M[a] Teresa Seisdedos with the fluorescence microscopy. We thank the technical works of A. Valencia and V. Morales. This work was supported by grants from the Comunidad Autónoma de Madrid (P-AMB-259-0505), the Comisión Interministerial de Ciencia y Tecnología (BIO2007-67304-C02, BIO2010-21049, CSD2007-00005) and by European Union Grants (GEN 2006-27750-C5-3-E and NMP2-CT-2007-026515).

References

Benjamini, Y., and Hochberg, Y. (1995) Controlling the false discovery rate: a practical and powerful approach to multiple testing. *J R Stat Soc B* **57:** 289–300.

Bustin, M., Catez, F., and Jae-Hwan, L. (2005) The dynamics of histone H1 function in chromatin. *Mol Cell* **17:** 617–620.

Caserta, E., Tomsic, J., Spurio, R., La Teana, A., Pon, C.L., and Gualerzi, C.O. (2006) Translation initiation factor IF2 interacts with the 30S ribosomal subunit via two separate binding sites. *J Mol Biol* **362:** 787–799.

de Eugenio, L.I., Galán, B., Escapa, I.F., Maestro, B., Sanz, J.M., García, J.L., and Prieto, M.A. (2010a) The PhaD regulator controls the simultaneous expression of the *pha* genes involved in polyhydroxyalkanoate metabolism and turnover in *Pseudomonas putida* KT2442. *Environ Microbiol* **12:** 1591–1603.

de Eugenio, L.I., Escapa, I.F., Morales, V., Dinjaski, N., Galán, B., García, J.L., and Prieto, M.A. (2010b) The turnover of medium-chain length polyhydroxyalkanoates in *Pseudomonas putida* KT2442 and the fundamental role of PhaZ depolymerase for the metabolic balance. *Environ Microbiol* **12:** 207–221.

de Lorenzo, V., and Timmis, K. (1994) Analysis and construction of stable phenotypes in gram-negative bacteria with Tn*5*- and Tn*10*-derived minitransposons. *Methods Enzymol* **235:** 386–405.

Deretic, V., and Konyecsni, W.M. (1990) A prokaryotic regulatory factor with a histone H1-like carboxy-terminal domain: clonal variation of repeats within *algP*, a gene involved in regulation of mucoid in *Pseudomonas aeruginosa*. *J Bacteriol* **172:** 5544–5554.

Deretic, V., Hibler, N.S., and Holt, S.C. (1992) Immunocytochemical analysis of AlgP (H_p1), a histonelike element participating in control of mucoidy in *Pseudomonas aeruginosa*. *J Bacteriol* **174:** 824–831.

Fasman, G.D. (ed.) (1976) *Handbook of Biochemistry and Molecular Biology. Section A. Proteins*, 3rd edn, Vol. **III**. Cleveland, OH: CRC Press.

Gerdes, K., Howard, M., and Szardenings, F. (2010) Pushing and pulling in prokaryotic DNA segregation. *Cell* **141:** 927–942.

Gitai, Z., Thanbichler, M., and Shapiro, L. (2005) The choreographed dynamics of bacterial chromosomes. *Trends Microbiol* **13:** 221–228.

Goyard, S. (1996) Identification of BpH2, a novel histone H1 homolog in *Bordetella pertussis*. *J Bacteriol* **178:** 3066–3071.

Grage, K., Jahns, A.C., Parlane, N., Palanisamy, R., Rasiah, I.A., Atwood, J.A., and Rehm, B.H. (2009) Bacterial polyhydroxyalkanoate granules: biogenesis, structure, and potential use as nano-/micro-beads in biotechnological and biomedical applications. *Biomacromolecules* **13:** 660–669.

Johnson, W.C., Jr (1988) Secondary structure of proteins through circular dichroism spectroscopy. *Annu Rev Biophys Biophys Chem* **17:** 145–166.

Kaniga, K., Delor, I., and Cornelis, G.R. (1991) A wide-host-range suicide vector for improving reverse genetics in gram-negative bacteria: inactivation of the *blaA* gene of *Yersinia enterocolitica*. *Gene* **109:** 137–141.

Kasinsky, H., Lewis, J., Dacks, J., and Ausio, J. (2001) Origin of H1 linker histones. *FASEB J* **15:** 34–42.

Kato, J., Tapan, M., and Chakrabarty, A.M. (1990) AlgR3, a protein resembling eukaryotic histone H1, regulates alginate synthesis in *Pseudomonas aeruginosa*. *Proc Natl Acad Sci USA* **87:** 2887–2891.

Kaul, R., Allen, M., Bradbury, E.M., and Wenman, W.M. (1996) Sequence specific binding of chlamydial histone H1-like protein. *Nucleic Acids Res* **24:** 2981–2989.

Kimberly, N.C., and Gitai, Z. (2010) Surface association and the MreB cytoskeleton regulate pilus production, localization and function in *Pseudomonas aeruginosa*. *Mol Microbiol* **76:** 1411–1426.

Komeili, A., Li, Z., Newman, D.K., and Jensen, G.J. (2006) Magnetosomes are cell membrane invaginations organized by the actin-like protein MamK. *Science* **311:** 242–245.

Koyama, Y., Katagiri, S., Hanai, S., Uchida, K., and Miwa, M. (1999) Poly (ADP-ribose) polymerase interacts with novel ribosomal proteins, L22 and L23a, with a unique histone-like amino-terminal extensions. *Gene* **226:** 339–345.

McCool, G.J., and Cannon, M.C. (1999) Polyhydroxyalkanoate inclusion body-associated proteins and coding region in *Bacillus megaterium*. *J Bacteriol* **181:** 585–592.

Madison, L.L., and Huisman, G.W. (1999) Metabolic engineering of poly (3-hydroxyalkanoates): from DNA to plastic. *Microbiol Mol Biol Rev* **63:** 21–53.

Medvedkin, V.N., Permyakov, E.A., Klimenko, L.V., Mitin, Y.V., Matsushima, N., Nakayama, S., and Kretsinger, R.H. (1995) Interactions of (Ala*Ala*Lys*Pro)n and (Lys*Lys*Ser*Pro)n with DNA. Proposed coiled-coil structure of AlgR3 and AlgP from *Pseudomonas aeruginosa*. *Protein Eng* **8:** 63–70.

Miller, W.G., and Lindow, S.E. (1997) An improved GFP cloning cassette designed for prokaryotic transcriptional fusions. *Gene* **191:** 149–153.

Moldes, C. (2003) Desarrollo de nuevos sistemas para la producción de proteínas de fusión por fermentación. PhD Thesis. Departamento de Microbiología II. Madrid: Universidad Complutense de Madrid (UCM).

Moldes, C., García, P., García, J.L., and Prieto, M.A. (2004) *In vivo* immobilization of fusion proteins on bioplastics by the novel tag BioF. *Appl Environ Microbiol* **70:** 3205–3012.

Nelson, K.E., Weinel, C., Paulsen, I.T., Dodson, R.J., Hilbert, H., Martins dos Santos, V.A.P., *et al*. (2002) Complete genome sequence and comparative analysis of the metabolically versatile *Pseudomonas putida* KT2440. *Environ Microbiol* **4:** 799–808.

Neumann, L., Spinozzi, F., Sinibaldi, R., Rustichelli, F., Pötter, M., and Steinbüchel, A. (2008) Binding of the major phasin, PhaP1, from *Ralstonia eutropha* H16 to poly (3-hydroxybutyrate) granules. *J Bacteriol* **190:** 2911–2919.

Niki, H., Yamaichi, Y., and Hiraga, S. (2000) Dynamic organization of chromosomal DNA in *Escherichia coli*. *Genes Dev* **14:** 212–223.

O'Leary, N.D., O'Connor, K.E., Ward, P., Goff, M., and Dobson, A.D. (2005) Genetic characterization of accumulation of polyhydroxyalkanoate from styrene in *Pseudomonas putida* CA-3. *Appl Environ Microbiol* **71:** 4380–4387.

Pieper-Fürst, U., Madkour, M.H., Mayer, F., and Steinbüchel, A. (1995) Identification of the region of a 14-kilodalton protein of *Rhodococcus ruber* that is responsible for the binding of this phasin to polyhydroxyalkanoic acid granules. *J Bacteriol* **177:** 2513–2523.

Prieto, M.A., Bühler, B., Jung, K., Witholt, B., and Kessler, B. (1999) PhaF, a polyhydroxyalkanoate-granule-associated protein of *Pseudomonas oleovorans* GPo1 involved in the regulatory expression system for *pha* genes. *J Bacteriol* **181:** 858–868.

Rehm, B.H. (2006) Genetics and biochemistry of polyhydroxyalkanoate granule self-assembly: the key role of polyester synthases. *Biotechnol Lett* **28:** 207–213.

Sambrook, J., and Russell, D.W. (2001) *Molecular Cloning. A Laboratory Manual*. Cold Spring Harbor, NY: CSHL Press.

Scheffel, A., Gruska, M., Faivre, D., Linaroudis, A., Plitzko, J.M., and Schuler, D. (2006) An acidic protein aligns magnetosomes along a filamentous structure in magnetotactic bacteria. *Nature* **440:** 110–114.

Scopes, R.K. (1974) Measurement of protein by spectrophotometry at 205 nm. *Anal Biochem* **59:** 277–282.

Smyth, G.K. (2004) Linear models and empirical Bayes methods for assessing differential expression in microarray experiments. *Stat Appl Genet Mol Biol* **3:** Article 3.

Smyth, G.K., and Speed, T. (2003) Normalization of cDNA microarray data. *Methods* **31:** 265–273.

Steinbüchel, A., and Hein, S. (2001) Biochemical and molecular basis of microbial synthesis of polyhydroxyalkanoates in microorganisms. *Adv Biochem Eng Biotechnol* **71:** 81–123.

Steinbüchel, A., Aerts, K., Babel, W., Follner, C., Liebergesell, M., Madkour, M.H., *et al*. (1995) Considerations on the structure and biochemistry of bacterial polyhydroxyalkanoic acid inclusions. *Can J Microbiol* **41:** 94–105.

Teleman, A.A., Graumann, P.L., Lin, D.C., Grossman, A.D., and Losick, R. (1998) Chromosome arrangement within a bacterium. *Curr Biol* **8:** 1102–1109.

Tian, J., Sinskey, A.J., and Stubbe, J. (2005) Kinetic studies of polyhydroxybutyrate granule formation in *Wautersia eutropha* H16 by transmission electron microscopy. *J Bacteriol* **187:** 3814–3824.

Timm, A., and Steinbüchel, A. (1992) Cloning and molecular analysis of the poly (3-hydroxyalkanoic acid) gene locus of *Pseudomonas aeruginosa* PAO1. *Eur J Biochem* **209:** 15–30.

Toy, K.E., Zhou, H., and Stephanopoulos, G.N. (2006) High-throughput screen for poly-3-hydroxybutyrate in *Escherichia coli* and *Synechocystis* sp. strain PCC6803. *Appl Environ Microbiol* **72:** 3412–3417.

Valentin, H.E., Stuart, E.S., Fuller, R.C., Lenz, R.W., and Dennis, D. (1998) Investigation of the function of proteins associated to polyhydroxyalkanoate inclusions in *Pseudomonas putida* BMO1. *J Biotechnol* **64:** 145–157.

Viollier, P.H., Thanbichler, M., McGrath, P.T., West, L., Meewan, M., McAdams, H.H., and Shapiro, L. (2004) Rapid and sequential movement of individual chromosomal loci to specific subcellular locations during bacterial DNA replication. *Proc Natl Acad Sci USA* **101:** 9257–9262.

Wieczorek, R., Pries, A., Steinbüchel, A., and Mayer, F. (1995) Analysis of a 24-kilodalton protein associated with the polyhydroxyalkanoic acid granules in *Alcaligenes eutrophus*. *J Bacteriol* **177:** 2425–2435.

Yang, Y.H., Dudoit, S., Luu, P., Lin, D.M., Peng, V., Ngai, J., and Speed, T.P. (2002) Normalization for cDNA microarray data: a robust composite method addressing single and multiple slide systematic variation. *Nucleic Acids Res* **30:** e15.

Yuste, L., Hervas, A.B., Canosa, I., Tobes, R., Jimenez, J.I., Nogales, J., *et al*. (2006) Growth phase-dependent expression of the *Pseudomonas putida* KT2440 transcriptional machinery analyzed with a genome-wide DNA microarray. *Environ Microbiol* **8:** 165–177.

Zlatanova, J., Caiafa, P., and van Holde, K. (2000) Linker histone binding and displacement: versatile mechanism for transcriptional regulation. *FASEB J* **14:** 1697–1704.

Supporting information

Additional supporting information may be found in the online version of this article.

Table S1. *P. putida* KT2442 vs *P. putida* KT42F DNA microarray data. RNA for microarray analyses was obtained from three independent cultures inoculated at 0.3 OD600 in PHA production medium and grown during 8h.

Fold Change	A	M	p. Value	FDR	ProbeID	Description
-27.35	11.81	-4.77	0.00000032	0.002	PP_5007	polyhydroxyalkanoate granule-associated protein GA2
-11.33	13.77	-3.5	0.00020395	0.062	PP_1149	hypothetical protein
-4.54	11.97	-2.18	0.00005636	0.041	PP_5282	ribosomal protein L28
-4.45	10.15	-2.15	0.00007362	0.041	PP_0600	ribosomal protein S20
-4.12	10.88	-2.04	0.00004004	0.041	PP_5087	ribosomal protein L31
-3.91	9.44	-1.97	0.00003296	0.041	PP_2036	dihydrodipicolinate synthase putative
-3.89	11.23	-1.96	0.00082003	0.103	PP_4116	isocitrate lyase
-3.71	9.09	-1.89	0.00002395	0.041	PP_5390	hypothetical protein
-3.64	9.64	-1.86	0.00008473	0.042	PP_0389	ribosomal protein S21
-3.45	10.93	-1.79	0.00067757	0.092	PP_5391	hypothetical protein
-3.39	10.17	-1.76	0.00044059	0.074	PP_1465	ribosomal protein L19
-3.26	10.14	-1.7	0.00005098	0.041	PP_5389	hypothetical protein
-3.25	9.63	-1.7	0.00055977	0.082	PP_4876	ribosomal protein S18
-3.01	9.73	-1.59	0.00036648	0.074	PP_4877	ribosomal protein S6
-2.93	9.59	-1.55	0.00054695	0.082	PP_4253	cytochrome c oxidase cbb3-type subunit III
-2.79	13.35	-1.48	0.00054105	0.082	PP_5008	polyhydroxyalkanoate granule-associated protein GA1
-2.77	11.49	-1.47	0.00013232	0.051	PP_1099	cold-shock domain family protein
-2.76	8.56	-1.46	0.00010277	0.046	PP_0504	outer membrane protein OprG
-2.42	11.3	-1.27	0.0007073	0.095	PP_0457	ribosomal protein L2
-2.39	10.45	-1.26	0.00023474	0.064	PP_0455	ribosomal protein L4
-2.35	11.14	-1.23	0.00022184	0.064	PP_2874	hypothetical protein
-2.35	9.61	-1.23	0.00015557	0.051	PP_5415	ATP synthase F1 alpha subunit
-2.28	9.14	-1.19	0.00020027	0.062	PP_1462	ribosomal protein S16
-2.28	10.79	-1.19	0.00021409	0.063	PP_1772	ribosomal protein S1
-2.22	8.59	-1.15	0.00032956	0.072	PP_0009	ribosomal protein L34
-2.2	10.44	-1.14	0.0003386	0.072	PP_5414	ATP synthase F1 gamma subunit
-2.19	11.36	-1.13	0.00030887	0.071	PP_2875	hypothetical protein
-2.17	11.94	-1.12	0.00073002	0.095	PP_0452	translation elongation factor Tu

-2.17	10.21	-1.12	0.00040728	0.074	PP_3050	pyocin R2_PP conserved hypothetical protein
-2.16	11.71	-1.11	0.00039809	0.074	PP_2467	ribosomal protein L35
-2.15	11.03	-1.1	0.00045938	0.075	PP_0469	ribosomal protein L6
-2.14	10.9	-1.1	0.0003158	0.071	PP_0454	ribosomal protein L3
-2.14	11.05	-1.1	0.00037181	0.074	PP_1315	ribosomal protein L13
-2.14	9.88	-1.1	0.00031129	0.071	PP_4185	succinyl-CoA synthetase alpha subunit
-2.09	9.19	-1.07	0.00060149	0.085	PP_4189	2-oxoglutarate dehydrogenase E1 component
-2.07	9.39	-1.05	0.00040564	0.074	PP_1592	translation elongation factor Ts
-2.02	9.24	-1.01	0.00046972	0.075	PP_1366	transcriptional regulator MvaT P16 subunit
-2.01	11.34	-1.01	0.00040027	0.074	PP_0468	ribosomal protein S8
-1.91	11.7	-0.94	0.0007342	0.095	PP_0458	ribosomal protein S19
2.07	10.93	1.05	0.00059243	0.084	PP_4364	anti-sigma F factor antagonist putative
2.09	11.2	1.06	0.00040446	0.074	PP_0550	conserved hypothetical protein
2.12	9.26	1.09	0.0005535	0.082	PP_4605	transcriptional regulator AraC family
2.17	11.38	1.12	0.00076162	0.097	PP_1991	hypothetical protein
2.27	10.82	1.18	0.00052962	0.082	PP_5365	cyclopropane-fatty-acyl-phospholipid synthase putative
2.3	11.75	1.2	0.00032127	0.071	PP_3832	carbon storage regulator
2.53	11.03	1.34	0.00011677	0.046	PP_2357	type 1 pili protein CsuB putative
2.54	11.23	1.34	0.0001121	0.046	PP_1814	conserved hypothetical protein
2.6	11.84	1.38	0.00044961	0.074	PP_4593	conserved hypothetical protein
3.43	10.68	1.78	0.00003918	0.041	PP_0837	conserved hypothetical protein
3.78	10.02	1.92	0.00003792	0.041	PP_4793	conserved hypothetical protein
3.83	11.63	1.94	0.00040909	0.074	PP_2118	conserved hypothetical protein
4.57	10.99	2.19	0.00007025	0.041	PP_3123	CoA-transferase subunit B putative
4.71	12.54	2.24	0.00004635	0.041	PP_4044	hypothetical protein
4.99	10.78	2.32	0.00004231	0.041	PP_3122	CoA-transferase subunit A putative
5.08	11.11	2.35	0.00007151	0.041	PP_2446	hypothetical protein
6.43	11.26	2.68	0.00014507	0.051	PP_4636	beta-ketothiolase
9.23	11.94	3.21	0.00000888	0.034	PP_1640	conserved hypothetical protein

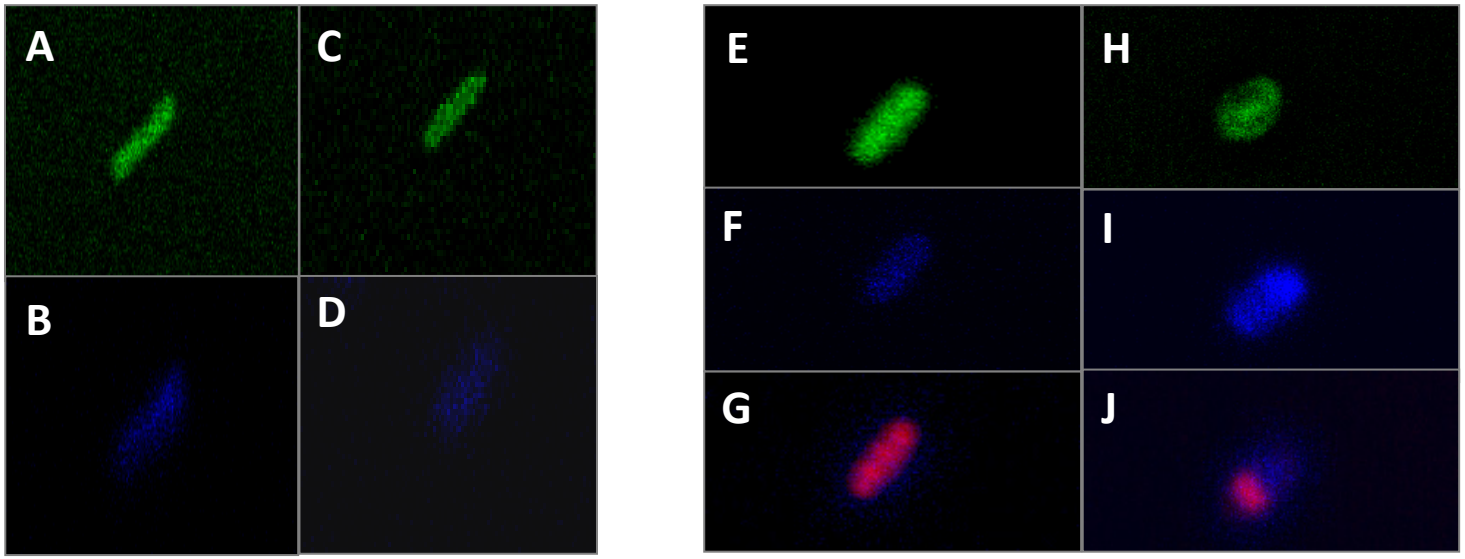

Fig. S1. *In vivo* localization of the C-terminal domain of PhaF, PHA granules and nucleoid in the wild type strain *P. putida* KT2442 and its PhaF minus mutant. A-D. Cells of KT42-GC (A, B) and KT42F-GC (C, D) grown overnight in LB expressing GFP::C-PhaF fusion protein: GFP (A, C), DAPI (B, D). E-J. Cells of KT42-GC (E-G) and KT42F-GC (H-J) grown in PHA granule producing conditions expressing GFP::C-PhaF fusion protein: GFP (E, H), DAPI (F, I) and Nile Red (G, J).